MGPB

One dimensional seismic response analysis at the non-commercial nuclear reactor site, Serpong - Indonesia

Rudarsko-geološko-naftni zbornik
(The Mining-Geology-Petroleum Engineering Bulletin)
UDC: 624:04 (author's propose)
DOI: 10.17794/rgn.2021.2.1

Original scientific paper

Yuliastuti Yuliastuti[1]; Heri Syaeful[2]; Arifan J. Syahbana[3]; Euis E. Alhakim[4]; Tagor M. Sembiring[5]

[1] *Center for Nuclear Energy System-National Nuclear Energy Agency (BATAN), Jl. Kuningan Barat, Mampang Prapatan, Jakarta, Indonesia, https://orcid.org/0000-0003-1328-8587*

[2] *Center for Nuclear Mineral Technology-National Nuclear Energy Agency (BATAN), Jl. Lebak Bulus Raya, Pasar Jumat, Jakarta, Indonesia, https://orcid.org/0000-0002-5478-0175*

[3] *Research Center for Geotechnology, Indonesian Institute of Sciences (LIPI), Bandung, Indonesia, https://orcid.org/0000-0003-2204-7355*

[4] *Center for Nuclear Energy System-National Nuclear Energy Agency (BATAN), Jl. Kuningan Barat, Mampang Prapatan, Jakarta, Indonesia, https://orcid.org/0000-0003-4026-1339*

[5] *Center for Nuclear Energy System-National Nuclear Energy Agency (BATAN), Jl. Kuningan Barat, Mampang Prapatan, Jakarta, Indonesia, https://orcid.org/0000-0003-4719-3615*

Abstract

One dimensional seismic response analysis on the ground surface of the Non-Commercial Power Reactor (RDNK) site based on the mean uniform hazard spectrum (UHS) and disaggregation analysis has been conducted. The study's objective was to perform an analysis on site-specific response spectra on the ground surface based on existing mean UHS and disaggregation data of the site that correspond to a 1,000 and 10,000 year return period of earthquakes in compliance with the national nuclear regulatory body requirements of Indonesia. Detailed site characterization was defined based on secondary data of a geotechnical drill-hole, seismic cross-hole, downhole data, and microtremor array data. The dynamic site characteristic analysis was presented along with strong motion selection and processing using two types of strong motion datasets. An investigation of strong motion selection, spectral matching, and scaling has been presented as an essential step in ground motion processing. One-dimensional equivalent linear analysis simulation was performed by computing the processed ground motions. A seismic design spectrum and ground surface response spectra from the two datasets of strong motion, both corresponding to a 10,000 and 1,000 year return period, are presented at the end of this study. This study has shown that in order to establish the appropriate seismic response design spectrum, site-specific data and seismic hazard analysis must be immensely considered.

Keywords:
input motion selection; nuclear site; seismic site response; Serpong

1. Introduction

In 2015, the National Nuclear Energy Agency (Badan Tenaga Nuklir Nasional, BATAN) had a plan to build a non-commercial nuclear power reactor (Reaktor Daya Non-Komersial, RDNK) based on a pebble-bed reactor high-temperature gas-cooled reactor (**Setiadipura, T. *et al.*, 2018**). The selected site is located near (less than 1 km distance) the Serpong Nuclear Complex inside the Center for Research, Science, and Technology (Pusat Pengembangan Ilmu Pengetahuan dan Teknologi, PUSPIPTEK) area. There are numerous and complex criteria for selecting a site for a nuclear reactor and other related facilities. For instance, to choose the location for the disposal of spent nuclear fuel (SNF), the site must comply with the geological, hydrogeological, hydrological, and other technical requirements (**Veinović, Z. *et al.*, 2019**). The criteria list for the nuclear reactor itself is longer than the SNF repository. At least seven aspects should be considered during site selection: seismic, volcanology, geotechnical, meteorology, hydrological, dispersion, and human-induced events.

Seismic hazard at the site became the primary concern in investigating the planned reactor's natural external hazard of the planned reactor because it is located within a relatively moderate seismic activity region and surrounded by a relatively dense population. Based on the 1900-2016 earthquake compilation catalogs (Incorporated Research Institutions for Seismology-IRIS; Meteorological, Climatological, and Geophysical Agency of Indonesia (Badan Meteorologi, Klimatologi, dan Geofisika, BMKG), and United States Geological Survey-USGS, there were at least four moderate scale earthquakes with a magnitude of 4-6Mw recorded within a 25

Corresponding author: Yuliastuti Yuliastuti
yuliastuti@batan.go.id

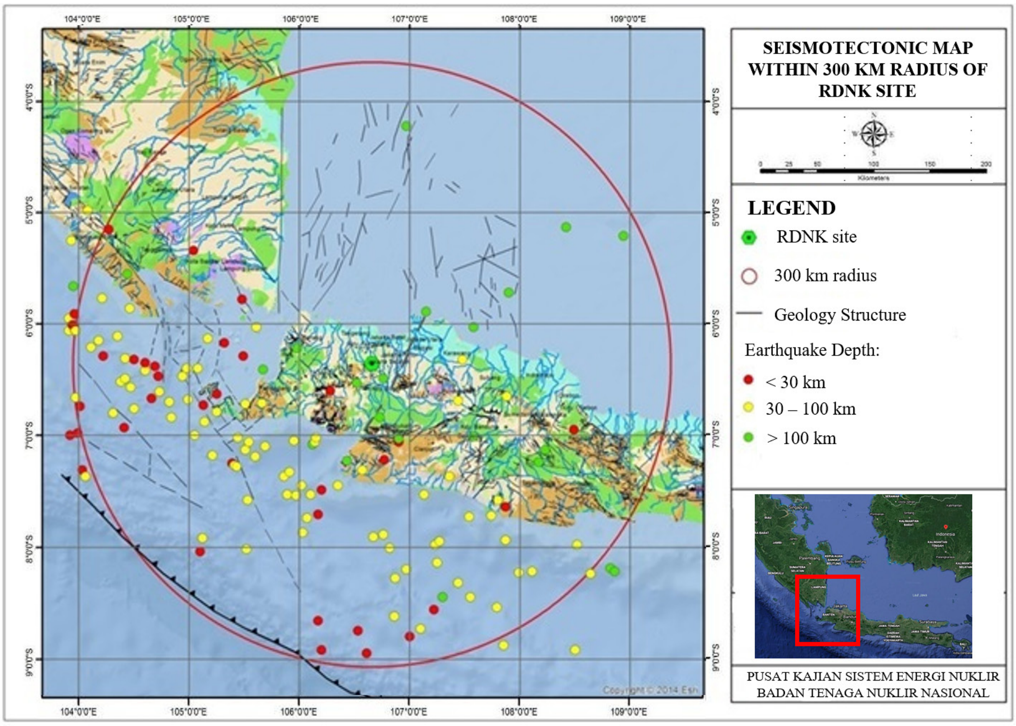

Figure 1: Seismotectonic map within 300 km radius of the RDNK Site
(Adapted from: **Badan Tenaga Nuklir Nasional, 2016**)

km radius from the site. The depth of these earthquakes was within 60 km down to 300 km. Probabilistic Seismic Hazard Analysis (PSHA) was performed within a 300 km radius from the site, as shown in **Figure 1**. Data for PSHA at the site shows a mean Uniform Hazard Spectrum (UHS) at the bedrock level was acquired from a previous study (**Badan Tenaga Nuklir Nasional, 2016**). The study also presented the disaggregation analysis corresponding to a 10,000 year return period, which complies with the national nuclear regulatory body regulation (**Badan Tenaga Nuklir Nasional, 2016**).

Stability of a structural system relies upon the shapes, sizes and the performance of the materials used (**Jaguljnjak Lazarević, A. *et al.*, 2017**). However, structural engineering design requires a comprehensive analysis of how earthquake characteristics on the ground surface affected the structure. It is well established that local soil conditions significantly affect the amplitude and response spectral characteristics of ground motions. **Suntoko, H. *et al.* (2019)** performed an analysis of the response design spectrum of RDNK reactor building. However, the study was done using only the mapped spectral response based on SNI 1726-2012 without considering the site-specific soil characteristics, PSHA and disaggregation analysis for the RDNK site. Indonesian National Standard (Standar Nasional Indonesia, SNI) 1726-2012 is the national standard that presents the design and construction criteria for general structures or buildings and could not be applied for specific or critical structures such as nuclear reactor installation. Thus, it was necessary to perform a site-specific investigation of design earthquake characteristics. This study's aim was to perform analyses on site-specific response spectra on the ground surface based on existing mean UHS and disaggregation data of the site that corresponds to a 1,000 and 10,000 year earthquake return period. The soil model for the equivalent linear analysis was developed using geological, geophysical, and geotechnical drill data. Previous study had performed preliminary analysis on spectral matching analysis at the site by using only Chi-Chi 1999 strong-motion dataset (**Yuliastuti, *et al.*, 2021**). Current analysis uses two datasets of strong motion, later called datasets A and B, which have different selection criteria. Dataset A was selected only by magnitude and distance, while dataset B was selected based on fault mechanism, magnitude, and distance.

2. Methods

In the following, the analysis of dynamic site characteristics is presented along with strong motion selection and processing using two strong motion datasets. An investigation of recorded strong motion selection, spectral matching, and scaling has been essential in strong-motion processing. One-dimensional equivalent linear analysis simulation was performed by computing the processed strong-motions, or later called input motions.

2.1. Generic soil model development

The RDNK site was situated between Banten Blok and southwest Java Basin (**Syaeful and Muhammad, 2017**).

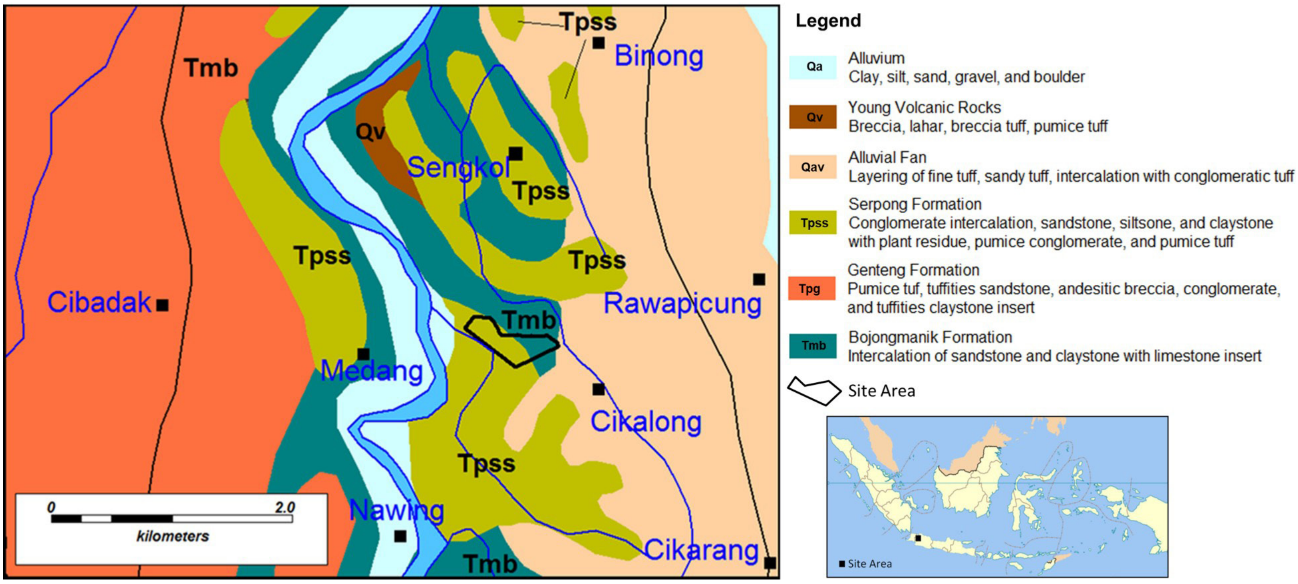

Figure 2: Geological map of RDNK site (Adapted from: **Sukardi T., 1992**)

Within a 300 km radius from the site area, several active faults have been identified, such as the Cimandiri, Lembang, Panaitan-Rajabasa and Mentawai faults (**Badan Tenaga Nuklir Nasional, 2016; Suntoko, H. *et al.*, 2019**). West Java was inundated in the Early Miocene period, which was then followed by the formation (Fm.) of the limestone of Rajamandala Fm. in the Oligocene period (**Syaeful and Muhammad, 2017**). Arc volcanism activity in the Early Miocene significantly occurred in south Java and stopped in the Middle Miocene period (**Clements, 2007**). Volcanogenic turbidite deposition in the northern part of Java island started in Late Miocene (**Clements, 2007**). Detailed geological field investigation of the Serpong site and the surrounding area by **Marjiyono *et al.* (2015)** showed that the lithological unit at the RDNK site includes limestone as a part of Bojongmanik Fm., tuff sandstone as part of Genteng Fm., conglomerate sedimentary rock as part of Serpong Fm., tuffs deposit, and alluvial sedimentary deposits (see **Figure 2**).

In developing ground surface response spectra, dynamic site analysis was performed using geotechnical and geophysical data, as shown in **Figure 3**. Geotechnical data used in this study consists of Standard Penetration Tests (SPT) (27 metre depth), a seismic cross-hole (100 metre depth), and downhole (50 metre depth) test data. **Seed *et al.* (1986),** as well as **Ohta and Goto (1978)** utilized empirical correlations of shear-wave velocity (V_s) and standard penetration test blow count (SPT), to acquire V_s from borehole data. Simultaneously, the geophysical data in the form of microtremor array was also used to cover a deeper soil profile. The shear-wave velocity profile for the soil model was developed based on the averaging approach. The soil model was generated based on the averaged V_s. Meanwhile, the lithology type for each layer was defined based on the geological coring and SPT results. A density log was used to determine the unit weight for each layer. From top to bottom, the soil model consists of a Serpong formation (topsoil, clay to silt, clayey to silty sand, and silty to clayey sand) and a Bojongmanik formation (Sandy claystone 3, Sandy claystone 2, Clayey sandstone, Sandy claystone 1, and Claystone). Topsoil in this model is the top layer of ground consisting of clay and organic materials. A generic one-dimensional soil model lithology column was generated consisting of nine soil layers, as shown in **Figure 4**.

A generic one-dimensional soil model, was then loaded into the DeepSoil code program (**Hashash *et al.*, 2016)** as such to produce a frequency range of 30-79 Hz. At least three input parameters were required: thickness, unit weight, and shear wave velocity for each layer of the soil model. The highest frequency was identified as a very thin layer of claystone at a depth of about 45 metres. The effective stress of the soil model tends to increase with depth, which also increases the rate of soil compression. A relatively high effective vertical stress was identified below 45 metres of depth, reaching 2000 KPa at the bottom of the soil model. The high-level of effective stress induced a high level of maximum strain as well.

The highest frequency is the maximum frequency that the layer can propagate and is calculated as given in **Equation 1 (Budhu, 2010)**. Meanwhile, total vertical stress (σ_v) at depth, z, is shown in **Equation 2 (Budhu, 2010)**. Effective vertical stress is equal to the total stress minus pore water pressure. Effective vertical stress is displayed in **Figure 5**, where the value of effective vertical stress is at the soil layer's mid-depth.

$$f_{\max} = \frac{V_s}{4d} \qquad (1)$$

Where:

V_s – the shear wave velocity of the layer (m/s),

d – the thickness of the layer (m).

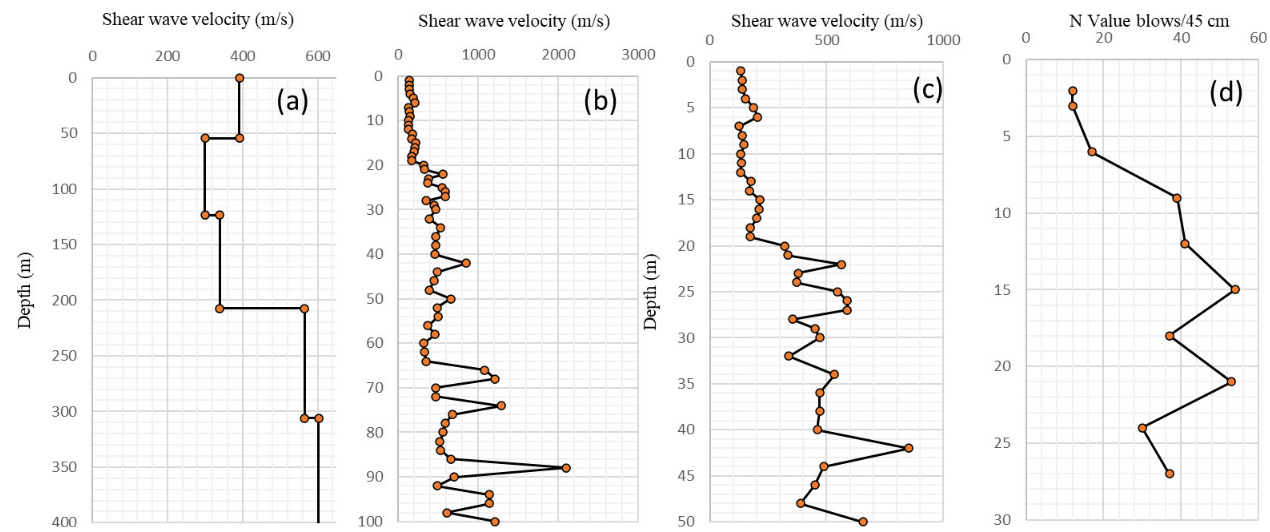

Figure 3: Shear-wave velocity profile. (a) microtremor array data. (b) seismic cross-hole test. (c) Shear-wave velocity profile based on seismic downhole test. (d) SPT N-value. (From: **Badan Tenaga Nuklir Nasional, 2016**)

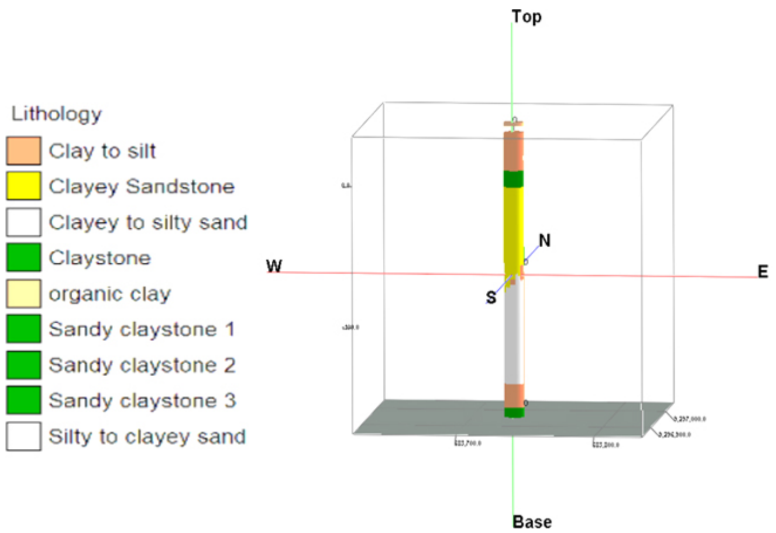

Layer #	Layer Name	Thickness (m)	Unit Weight (kN/m³)
1	Top Soil	2.5	15.69
2	Clay to silt	4.55	15.69
3	Clayey to silty sand	5.8	14.81
4	Silty to clayey sand	10.87	15.89
5	Sandy Claystone 3	10.04	13.44
6	Sandy Claystone 2	10.49	12.75
7	Clayey Sandstone	1.36	13.34
8	Sandy claystone 1	6.215	12.36
9	Claystone	156.175	16.08

Figure 4: A one-dimensional soil model of the RDNK site based on data averaging of geotechnical and geophysical data. The left picture shows the lithology column. The right table shows the thickness and unit weight parameters used.

$$\sigma_v = \gamma_1 d_1 + \gamma_2 (d_2) + \ldots + \gamma_n (z - d_1 - \ldots d_n) \qquad (2)$$

Where:

γ_1, γ_2, γ_n – the unit weight for each soil layer.

The input parameters required to perform site response analysis on the ground surface are damping and modulus reduction curves for each layer of the soil profile. The selection of the curves was based on the soil and rock characteristics of each layer. **Seed *et al.* (1986)**, **Vucetic and Dobry (1991)**, and EPRI 250-500 (**Pyke and North, 1973**) modulus and damping curves were applied to each of the soil layer based on the lithology class and secondary data of soil laboratory test. **Figure 6** shows the material modulus and damping reference curves.

2.2. Input motion selection and scaling

Seismic hazard disaggregation analysis is a process to determine the dominant earthquake Magnitude (Mw) and rupture distance (R), which significantly contributes to the probabilistic seismic hazard analysis of the site at a specific return period. The disaggregation analysis of the RDNK site resulting in a dominant hazard coming from the subduction regime (Normal fault mechanism) with a mean magnitude of 7.88 Mw and a mean distance of 122.28 km **(Badan Tenaga Nuklir Nasional, 2016)**. Based on this analysis, strong motions were selected.

A dataset of strong-motion data was acquired through several strong-motion databases such as NGA West **(Ancheta *et al.*, 2014)**, Center for Engineering Strong Motion Data (CESMD), and K-NET. All selected strong motions were located on the outcrop and consist of horizontal and vertical components. Input motion spectral matching and scaling were performed only for the horizontal component. In this study, a comparison of two types of strong motion selection were presented. The first type of selection, later called A, was conducted by

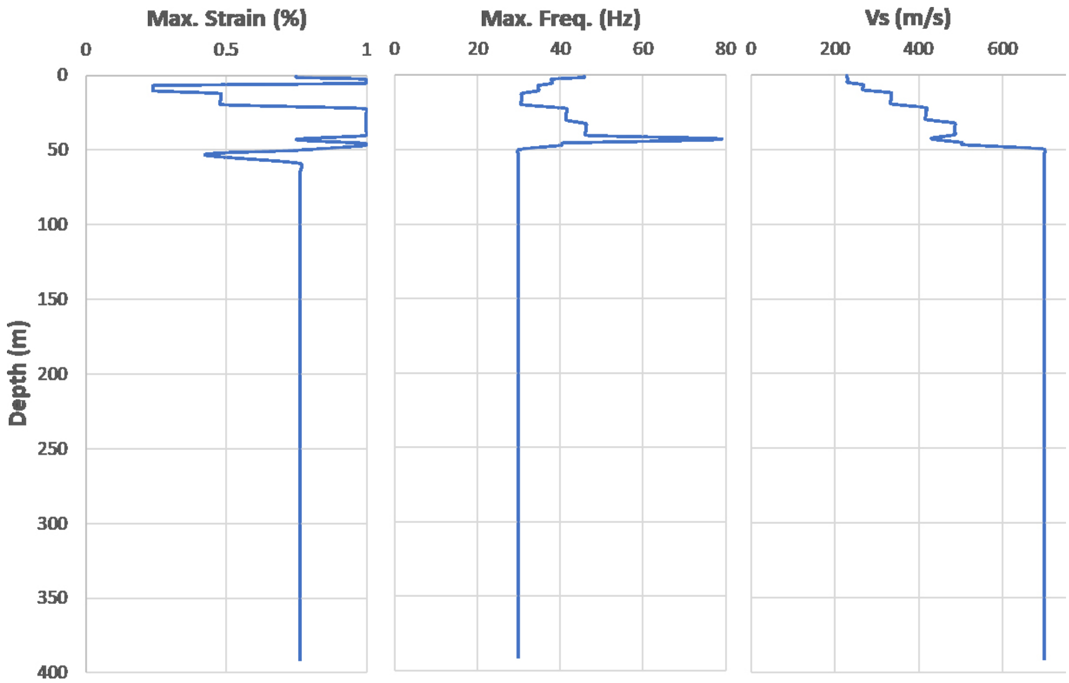

Figure 5: Strain (%) (left), Maximum frequency (Hz) (centre) and shear wave velocity (right) profile with depth (m)

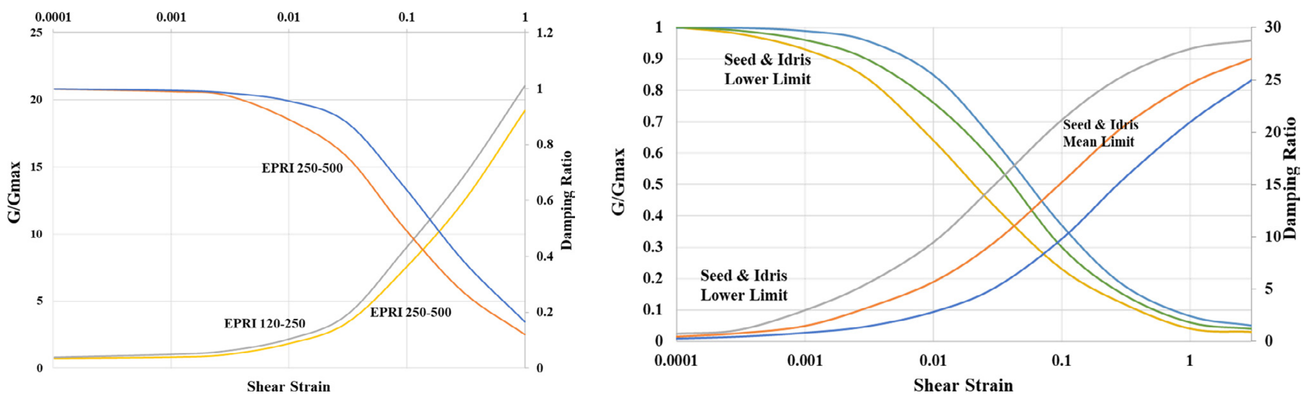

Figure 6: Material reference curve. The left side is the material reference curve using Seed & Idris for Lower, Mean and Upper limit. The right side is the material reference curve using EPRI standard corresponding for depth 120-250 metres and 250-500 metres. (From: **Sun, Golesorkhi and Seed (1972)** and **Pyke and North (1973)**).

considering all kinds of tectonic regimes, regardless of the fault mechanism, within the range of magnitude and distance based on disaggregation analysis, as mentioned before. **Table 1** lists the selected strong motions based on this type of selection, consisting of active shallow crustal and megathrust/subduction interface tectonic regimes. The second type, later called B, was to select strong motions strictly based on fault mechanism (Normal/Reverse) and magnitude and distance following the disaggregation analysis result. Five strong motions have been selected based on this type of selection, as shown in **Table 2**.

Despite the out of range magnitude, the Tohoku earthquake (2011) was also utilized as the input motions for both of the ground motion selection types to consider the possibility of a 9 Mw earthquake at the Java megathrust as stated in the Indonesian National Standard 03-1726-2002. The 9.1 Mw Tohoku earthquake was one of the earthquake events that happened on the subduction interface.

Spectral matching and scaling processes were applied to each of the strong motions by preserving the non-stationary properties of the original accelerogram using Al Atik & Abrahamson algorithm available on Seismomatch 2020. The result of spectral matching and scaling for ground motions dataset A and B correspond to a 10,000 year and 1,000 year return period (see **Figure 7**).

As shown in **Table 2**, the ground motion dataset B consisted of the El Salvador (2001) earthquake due to the compatibility of its magnitude, distance, and source mechanism. Nevertheless, this particular earthquake generated a high rise to the spectral matching misfit

Table 1: Strong-motions dataset A

Tectonic Regime	Earthquake	Station	Fault Mechanism	Year	Magnitude (Mw)	Epicenter Distance (km)	Depth (km)
Subduction	Chi-Chi, Taiwan	TAP069	RV-OBL	1999	7.62	123.57	11
Active Shallow Crustal	Tabas, Iran	Bajesten	RV	1978	7.35	120.81	10
Subduction	Tohoku	MYG013	RV	2011	9.1	170	29
Active Shallow Crustal	Kocaeli, Turkey	Eregli	SS	1999	7.51	142.29	17
Active Shallow Crustal	Denali, Alaska	Fairbanks University of Alaska	SS	2002	7.9	139.69	4.9
Active Shallow Crustal	Kocaeli, Turkey	Botas	SS	1999	7.51	127.05	17
Subduction	Kepulauan Mentawai Region	CTO Station PSKI	RV	2007	7.9	164.6	35
Subduction	Limon, Costa Rica	Quepos, CSMIP station 80066	Thrust	1991	7.7	121	22

Note: SS:Strike-slip; RV: Reverse; RV-OBL: Reverse-Oblique

Table 2: Strong-motions dataset B

Tectonic Regime	Earthquake	Station	Fault Mechanism	Year	Magnitude (Mw)	Epicenter Distance (km)	Depth (km)
Subduction	Chi-Chi, Taiwan	TAP069	RV-OBL	1999	7.62	123.57	11
Subduction	Tohoku	MYG013	RV	2011	9.1	170	29
Subduction	Kepulauan Mentawai Region	CTO Station PSKI	RV	2007	7.9	164.6	35
Subduction	Limon, Costa Rica	Quepos, CSMIP station 80066	Thrust	1991	7.7	121	22
Shallow background	El Salvador	UCA station TO	Normal	2001	7.6	105.7	60

reaching a 192% maximum misfit. Thus, the El Salvador (2001) earthquake was eliminated from the ground motion dataset B. Baseline correction was applied to all the selected input motions to avoid time series drifting. As stated in **Boore (1999)**, a good baseline correction to maintain the actual real signal was required. Amplitude shifting at low and high frequency was noticeably due to the baseline correction process.

Baseline correction was applied to all the selected input motions to avoid time series drifting. **Figure 7** shows one example of a baseline correction application on Kepulauan Mentawai (2007) ground motion. The blue line shows the original motion data, while the purple line shows the baseline-corrected data. Fourier spectra comparison before and after baseline correction yielded 2834 correction points. Amplitude shifting at low and high frequency was noticeable due to the baseline correction process.

3. Results

One-dimensional total stress analysis using equivalent linear analysis in the frequency domain was conducted using DeepSoil codes (**Hashash *et al.*, 2016)**. Baseline corrected strong motions were utilized as the input motions for the equivalent linear analysis. Based on the input motion type used in this study, elastic half-space was utilized to characterize the bedrock. The bedrock properties included at least three parameters, namely Vs, unit weight, and damping ratio. According to the geophysical data, Vs of 750 m/s, unit weight of 18.36 kN/m3, and 5% damping ratio was assigned as the bedrock properties.

Iteration for the analysis was performed fifteen times to get the convergence value. The input enabled the program to calculate initial shear modulus by correlating shear wave velocity and unit weight. Iterated shear modulus was calculated based on the frequency-dependent complex shear modulus formulation, which relates the shear modulus initial to shear modulus iterated by using the damping ratio **(Hashash *et al.*, 2016)**. The initial damping ratio was calculated based on selecting the damping curve, as mentioned in the previous chapter of dynamic site characteristics.

Spectral acceleration for each input motion has been plotted over the seismic design spectrum in **Figure 9**,

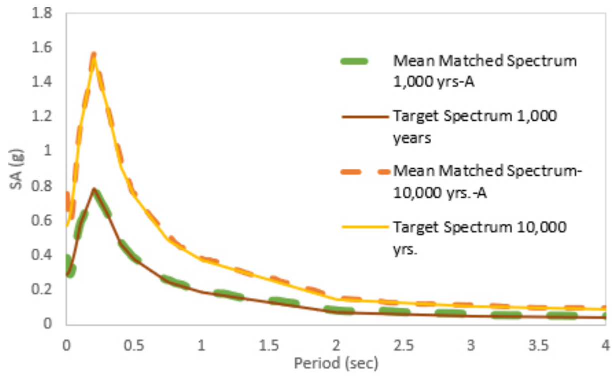

	10,000 yrs.	1,000 yrs.
Ave. misfit	5.29%	9.61%
Max. misfit	12.03%	25.29%
Max. Acceleration	1.56g	0.79g

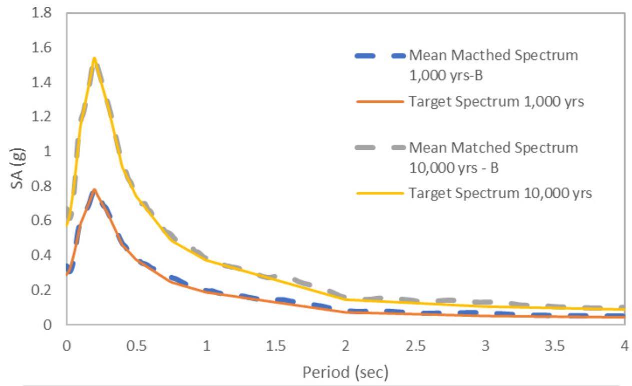

	10,000 yrs.	1,000 yrs.
Ave. misfit	9.89%	10.39%
Max. misfit	27.34%	30.68%
Max. Acceleration	1.54g	0.79g

Figure 7: Spectral matching result for ground motion dataset A (left-side) and ground motion dataset B (right-side). The lower table shows the average and maximum misfit resulted from the spectral matching process. Maximum acceleration is the maximum calculated acceleration from the selected strong motion.

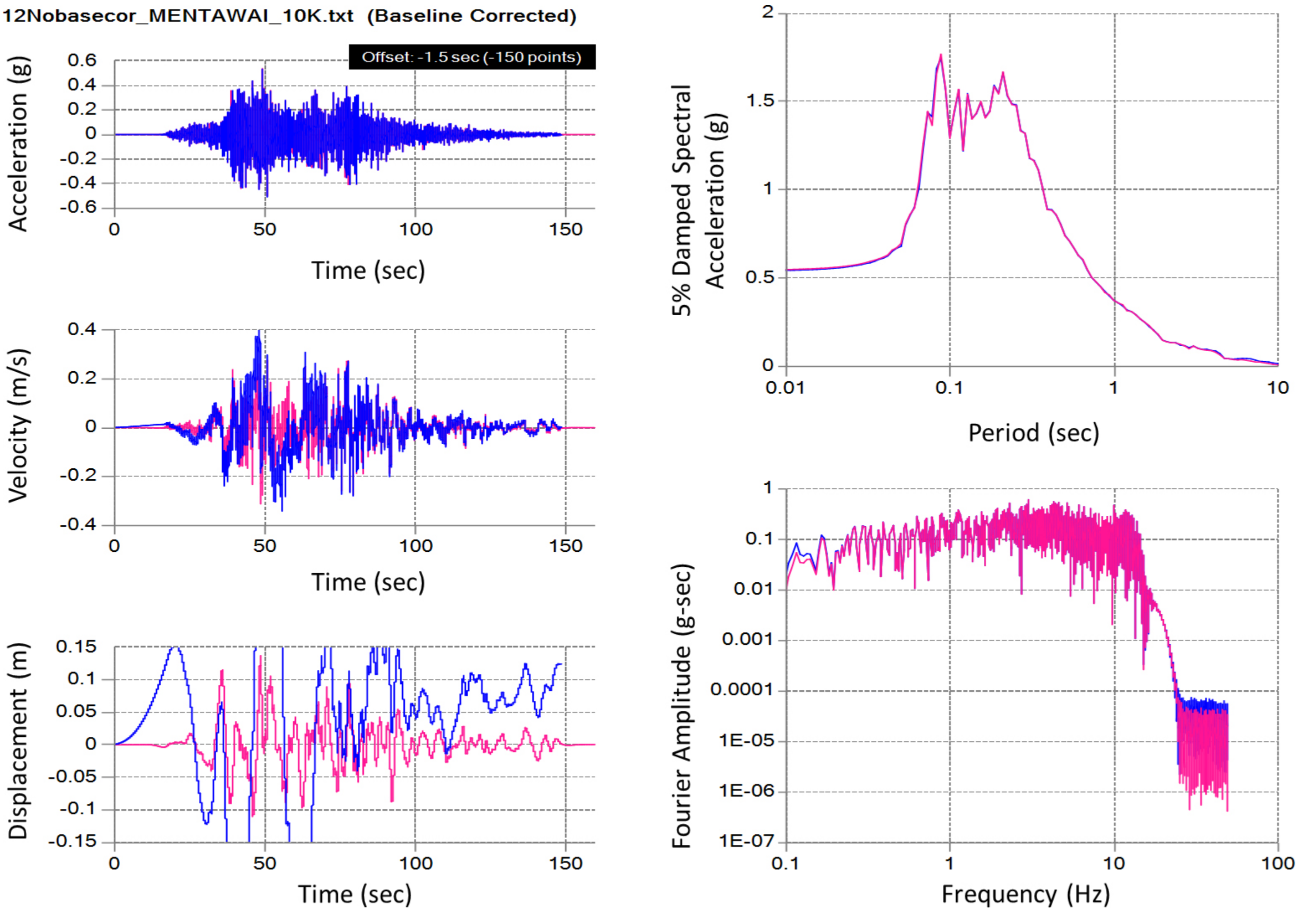

Figure 8: Baseline correction application on Mentawai ground motion. (a) Comparison of original time series with baseline corrected data. (b) Spectral Acceleration comparison of original ground motion data and baseline corrected data. (c) Fourier spectra comparison of original ground motion data and baseline corrected data.

both corresponding to a 10,000 and 1,000 year return period. The design spectrum was developed following the Indonesian National Standard 03-1726-2002 on "Procedures on Earthquake Resistance Planning for Buildings" and ASCE 7-10. The seismic design spectrum parameters are shown in **Table 3**.

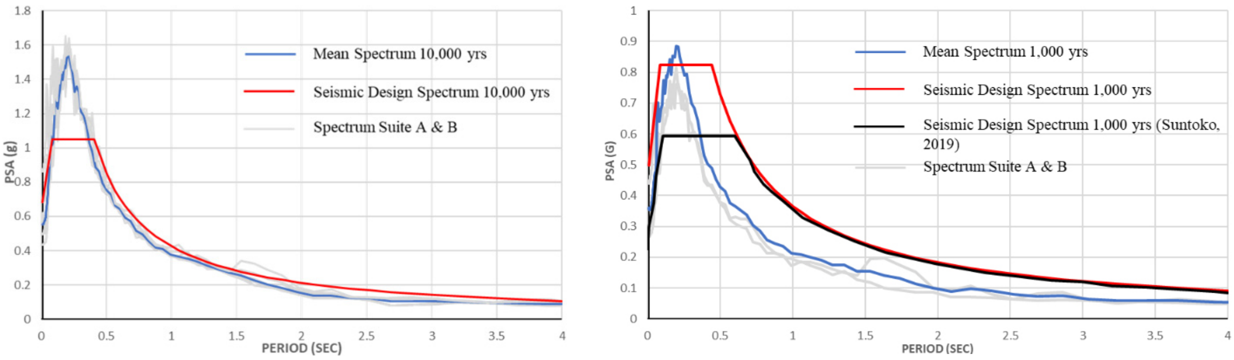

Figure 9: Spectral acceleration on the ground surface corresponds to a 10,000 year return period (left) and a 1,000 year return period (right). Mean Spectrum is the average spectral acceleration value from each strong-motion dataset. Spectrum datasets A & B were the mean spectrum for each selected strong motion. The right-side picture also presents a comparison of the resulting seismic design spectrum with the previous study from **Suntoko *et al.* (2019)**.

Table 3. Recommended seismic design spectrum over a 10,000 year and 1,000 year return period.

Para-meters	Unit	10,000 years		1,000 years	
		Dataset A	Dataset B	Dataset A	Dataset B
S_s	g	1.57	1.59	1.08	1.24
S_1	g	0.39	0.38	0.27	0.31
F_a	-	1.00	1.00	1	1
F_v	-	1.62	1.64	1.86	1.78
S_{D1}	g	0.43	0.41	0.34	0.37
S_{M1}	g	0.64	0.62	0.51	0.55
S_{DS}	g	1.05	1.06	0.72	0.82
S_{MS}	g	1.57	1.59	1.08	1.24
T_0	sec	0.08	0.08	0.09	0.09
T_S	sec	0.41	0.39	0.47	0.44

to each input motion corresponding to both, a 10,000 and 1,000 year return period. The soil amplification factor corresponds to a 10,000 year return period for dataset A, and B, and yields 1.65 and 1.67, respectively. Meanwhile, for a 1,000 year return period, the soil amplification factors were 1.69 and 1.68, respectively, for datasets A and B.

4. Discussion

For a 10,000 year return period, maximum pseudo-spectral acceleration of the input motions at a short period range (T = 0.2 - 1 sec) was contributed by the Mentawai, Indonesia (2007) input motion, which yields 1.7678g. This particular earthquake is categorized as a shallow earthquake caused by a thrust faulting on the boundary plate of Indo-Australia and the Sunda plate (**Hayes, G.P., et al., 2017**). Meanwhile, at a longer-period (T > 1.5 sec), Tohoku (2011) input motion has a clear offset from the rest of the datasets. This phenomenon is because the large magnitude and distant earthquake(s) tend to have a moderate response spectra peak at a short period and a much higher peak at a longer period compare to the moderate magnitude and close earthquake.

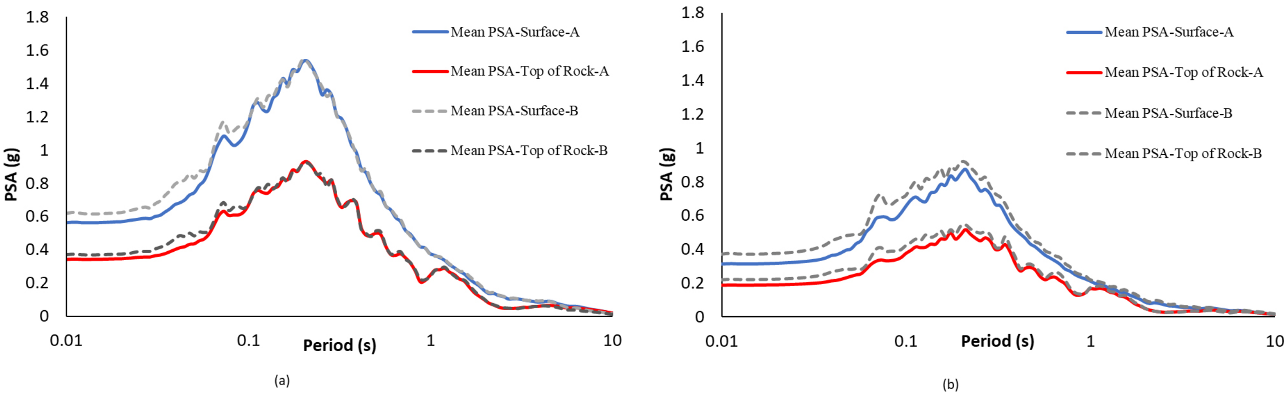

Figure 10: Comparison of top of rock and surface layer response spectra corresponds to a 10,000 year (a) and a 1,000 year return period (b)

Figure 10 shows the mean spectra comparison of the top of rock layer and surface layer. The top of rock is defined at the bottom of soil model (Claystone with a unit weight of 16.08 kN/m^3 and V_s of 698 m/s). The surface layer is defined as the topsoil layer (Clay and organic material with a unit weight of 15.69 kN/m^3 and V_s of 229 m/s. The spectra were built based on pseudo-spectral acceleration data for each layer when subjected

For both a 10,000 and 1,000 year return period, the mean response spectra of dataset B yield a higher value than strong-motion dataset A, resulting in a slightly different seismic design spectrum parameter. UHS at bedrock was utilized to determine some of the seismic design spectrum parameters, especially spectral acceleration at a period of 0.2 sec (S_s) and 1 sec (S_1). Spectral response acceleration at the ground surface for a 1,000 and 10,000 year return period as displayed in **Figure 9** shows that at short period ranges and a 1 sec period, dataset A gives a 6% lower value compare to dataset B.

A previous study by **Suntoko, H. *et al.* (2019)** had generated the seismic design response spectrum corresponding to a 1,000 year return period with S_1 = 0.3 g, S_S = 0.75 g, and S_{DS} = 0.6 g. Comparing these coefficients obtained from **Suntoko, H. *et al.* (2019)** with the current result in **Table 3**, it gives a 22-32% higher value in terms of the S_{DS} coefficient, and 33-49% for the S_S coefficient. Whereas, the S_1 coefficient tends to be 1-3% lower than **Suntoko, H. *et al.* (2019)**. The different seismic design response coefficients create a significant impact to the civil design of the reactor and other buildings in the site area.

Seismic hazard analysis of a building structure cannot be carried out simply based on the maximum value of ground acceleration. Ground motion frequency content and dynamic soil properties influence the kind of response generated by the structure. The mean spectra on the ground surface reveals that the probability of ground motion exceedance level produces a significant difference to the resulted seismic response spectra.

5. Conclusions

Regional-scale seismic hazard analysis and site-specific data are essential to acquire a reliable seismic response design spectrum at the ground surface. Mean UHS resulted from a regional seismic hazard study has been utilized in this study. The mean UHS was assigned as the target spectrum when performing spectral matching and scaling. Eleven recorded strong-motions were selected based on the disaggregation analysis at the site. The calculation shows that, at the ground surface, peak ground acceleration (PGA) for a 10,000 and 1,000 year return period are in the range of 0.59-0.61g and 0.38-0.4g, respectively.

A significant finding to emerge from this study is that the generated design response spectrum differs from previous study results **(Suntoko H., *et. al* 2019)**, which did not include the soil profile and detailed site seismic hazard analysis. The utilization of seismic hazard and site-specific data give a 22-32% higher value in terms of the S_{DS} coefficient, 33-49% for the S_S coefficient, and 1-3% lower of the S_1 coefficient compared with **Suntoko (2019)**.

Besides, the selection criteria of input motion produce a different result of the ground surface's spectral response. Dataset A is comprised of eight selected strong-motions without considering the source mechanism or fault type. Meanwhile, dataset B consists of five strong-motions selected based on fault type, magnitude, and source distance. The calculation shows that dataset B gives a 6% higher peak ground acceleration compared to dataset A.

Acknowledgment

The funding for this research was provided by the annual budget of the Center for Nuclear Energy System Assessment (Pusat Kajian Sistem Energi Nuklir, PKSEN-BATAN) for the year 2020. This support is gratefully acknowledged. We are also thankful to BMKG, National Center for Earthquake Study (Pusat Studi Gempa Nasional, PUSGEN), and Research Center for Human Settlement (Pusat Litbang Perumahan dan Permukiman, PUSKIM) for providing the necessary data and analyses.

6. References

Ancheta, T. D. et al. (2014): NGA-West2 Database. Earthquake Spectra, 30(3), 989–1005. doi: 10.1193/070913EQS197M.

Badan Tenaga Nuklir Nasional (2016): Laporan Evaluasi Tapak III.A.3 Geoteknik dan Pondasi Rev.4, Pusat Kajian Sistem Energi Nuklir, Badan Tenaga Nuklir Nasional, Jakarta. (*in Bahasa Indonesia, no English Abstract*)

Boore, D. M. (1999): Effect of Baseline Correction on Response Spectra for Two Recordings of the 1999 Chi-Chi, Taiwan, Earthquake. Bulletin of the Seismological Society of America, 91(October), 1119–1211. doi: https://doi.org/10.3133/ofr99545.

Budhu, M. (2010): Soil Mechanics and foundations. John Wiley & Sons, Chichester, 761 p.

Clements, B. (2007): Cretaceous to Late Miocene Stratigraphic and Tectonic Evolution of West Java. In Proceedings, Indonesian Petroleum Association 31st Annual Convention. Jakarta. doi: 10.29118/ipa.1520.07.g.037.

Hashash, Y. M. A. et al. (2016): DeepSoil 6.1 User Manual. University of Illinois, 137 p.

Hayes, G.P., Myers, E.K., Dewey, J.W., Briggs, R.W., Earle, P.S., Benz, H.M., Smoczyk, G.M., F. and H.E., Barnhart, W.D., Gold, R.D., and Furlong, K. P. (2017): Tectonic Summaries of Magnitude 7 And Greater Earthquakes From 2000 to 2015. U.S. Geological Survey Open-File Report 2016-1192. http://www.usgs.gov.

Jaguljnjak Lazarević, A., Uroš, M., & Čengija, A. (2017). Fundamental models of structural stability. The Mining-Geological-Petroleum Engineering Bulletin (Rudarsko-geološko-Naftni Zbornik), 32, 2, 37–47.

Marjiyono, M. et al. (2015): Kelas Soil Daerah Sekitar Rencana Tapak Reaktor Daya Eksperimental (Rde) Serpong Dari Data Mikrotremor, Jurnal Pengembangan Energi Nuklir, 17(1), 57. doi: 10.17146/jpen.2015.17.1.2591. *(in Bahasa Indonesia –Abstract in English)*

Ohta, Y. and Goto, N. (1978): Empirical Shear Wave Velocity Equations in Terms of Characteristic Soil Indexes. Earthquake Engineering & Structural Dynamics. John Wiley & Sons, Ltd, 6(2), 167–187. doi: 10.1002/eqe.4290060205.

Pyke, R. and North, J. (1973): Modeling of Dynamic Soil Properties, Appendix 7.A, Guidelines for Determining Design Basis Ground Motions. EPRI report No. TR-102993. http://www.resolutionmineeis.us/sites/default/files/references/epri-1993.pdf.

Seed, H. B. et al. (1986): Moduli and Damping Factors for Dynamic Analyses of Cohesionless Soils. Journal of Geotechnical Engineering, 112(11), 1016–1032. doi: 10.1061/(ASCE)0733-9410(1986)112:11(1016).

Setiadipura, T. et al. (2018): Cooling Passive Safety Features of Reaktor Daya Eksperimental. In AIP Conference Proceedings 1984, 020034. doi: 10.1063/1.5046618.

Sukardi, T. (1992): Peta Geologi Lembar Jakarta dan Kepulauan Seribu Skala 1:100.000. Bandung.

Sun, J. I., Golesorkhi, R. and Seed, H. B. (1972): Dynamic Moduli and Damping Ratios for Cohesive Soils. Journal of Terramechanics, 1-46. doi: 10.1016/0022-4898(72)90024-9.

Suntoko, H. et al. (2019): Analisis Spektrum Respon Desain Gedung Reaktor RDE Menggunakan SAP2000. Jurnal Pengembangan Energi Nuklir, 21(1), pp. 1–7. *(in Bahasa Indonesia)*

Syaeful, H. and Muhammad, A. G. (2017): Interpretasi Lingkungan Pengendapan Formasi Batuan Menggunakan Analisis Elektrofasies di Lokasi Tapak Puspiptek Serpong. Eksplorium, 38, 1, 29. doi: 10.17146/eksplorium.2017.38.1.3538.

Veinović, Želimir, Uroić, G., Domitrović, D., & Kegel, L. (2019). Thermo-hydro-mechanical effects on host rock for a generic spent nuclear fuel repository. The Mining-Geological-Petroleum Engineering Bulletin (Rudarsko-geološko-Naftni Zbornik), 35, 1, 65-80. doi: 10.17794/rgn.2020.1.6

Vucetic, M. and Dobry, R. (1991): Effect of Soil Plasticity on Cyclic Response. Journal of Geotechnical Engineering, 117, 1, 89–107. doi: 10.1061/(ASCE)0733-9410(1991)117:1(89).

Yuliastuti, et al. (2021): Preliminary Spectral Matching Analysis of RDE site at Serpong Indonesia. Journal of Physics: Conference Series 1772 (2021) 012028. doi: 10.1088/1742-6596/1772/1/012028

SAŽETAK

Jednodimenzionalna analiza seizmičkih vrijednosti na smjestištu nekomercijalnoga nuklearnog reaktora, Serpong, Indonezija

Jednodimenzionalna seizmička analiza na tlu u okolici nekomercijalnoga nuklearnog reaktora temeljena je na izučavanju srednjih, uniformnih spektara rizika te analizi dezagregacije tla. Analiza je načinjena na smjestištu koje je određeno svojim posebnim seizmičkim spektrom. Spomenute varijable izučavane su s obzirom na povratno razdoblje potresa od 1000 i 10 000 godina te su uspoređene s nacionalnim zakonodavstvom o sigurnosti nuklearnih postrojenja u Indoneziji. Analizirano područje detaljno je opisano iz sekundarnih podataka koji su obuhvatili geotehničke i sezimičke bušotinske podatke te mjerenja mikropotresa. Dinamička svojstva smjestišta predstavljena su usporedno s podatcima iz dvaju skupova mjerenja snažnih gibanja. Njihovo izučavanje spektralnom analizom te odabirom mjerenja opisano je kao temeljni korak u izučavanju gibanja tla. Jednodimenzionalna analiza načinjena je računalnom obradbom. Prikazani su seizmički i površinski spektri, za oba skupa podataka i oba povratna razdoblja. Pokazano je kako ove metode trebaju nužno biti korištene u analizi seizmičkoga rizika na smjestištima ove vrste.

Ključne riječi:
odabir ulaznoga gibanja; nuklearno postrojenje; seizmički odgovor; Serpong

Author’s contribution

Yuliastuti Yuliastuti (1) (Researcher, MSi, Geophysics) provided the data processing and the analysis of generic soil model development and input motion processing as well as the interpretation of the results. **Heri Syaeful (2)** (Researcher, MT, Geology) participated in field work, conducted sample preparation and measurement and contributed with the geology of Serpong site. **Arifan J. Syahbana (3)** (Researcher, PhD candidate, Civil Engineering) participated in seismic response analysis simulation and interpretation. **Euis E. Alhakim (4)** (Researcher, S.Si, Geography) contributed with the development of soil model and map construction. **Tagor M. Sembiring (5)** (Senior Researcher, Ir., Nuclear Engineering) provided the statistic analysis and nuclear safety analysis of the results.